

## Article

# Reliability-Based Robust Design Optimization for Maximizing the Output Torque of Brushless Direct Current (BLDC) Motors Considering Manufacturing Uncertainty

Kyunghun Jeon <sup>1</sup>, Donghyeon Yoo <sup>1</sup>, Jongjin Park <sup>1</sup>, Ki-Deok Lee <sup>2</sup> , Jeong-Jong Lee <sup>2</sup> and Chang-Wan Kim <sup>3,\*</sup> 

- <sup>1</sup> Graduate School of Mechanical Design & Production Engineering, Konkuk University, 120 Neungdong-ro, Gwangjin-gu, Seoul 05029, Korea
- <sup>2</sup> Intelligent Mechatronics Research Center, Korea Electronics Technology Institute, Seongnam-si 13509, Gyeonggi-do, Korea
- <sup>3</sup> School of Mechanical Engineering, Konkuk University, 120 Neungdong-ro, Gwangjin-gu, Seoul 05029, Korea
- \* Correspondence: goodant@konkuk.ac.kr

**Abstract:** In recent years, the deterministic design optimization method has been widely used to improve the output performance of brushless direct current (BLDC) motors. However, it does not contribute to reducing the failure rate and performance variation of products because it cannot determine the manufacturing uncertainty. In this study, we proposed reliability-based robust design optimization to improve the output torque of a BLDC motor while reducing the failure rate and performance variation. We calculated the output torque and vibration response of the BLDC motor using the electromagnetic–structural coupled analysis. We selected the tooth thickness, slot opening width, slot radius, slot depth, tooth width, magnet thickness, and magnet length as the design variables related to the shape of the stator and rotor that affect the output torque. We considered the distribution of design variables with manufacturing tolerances. We performed a reliability analysis of the BLDC motor considering the distribution of design variables with manufacturing tolerances. Using the reliability analysis results, we performed reliability-based robust design optimization (RBRDO) to maximize the output torque; consequently, the output torque increased by 8.8% compared to the initial BLDC motor, the standard deviation in output performance decreased by 46.9% with improved robustness, and the failure rate decreased by 99.2% with enhanced reliability. The proposed reliability-based robust design optimization is considered to be useful in the actual product design field because it can evaluate both the reliability and robustness of the product and improve its performance in the design stage.



**Citation:** Jeon, K.; Yoo, D.; Park, J.; Lee, K.-D.; Lee, J.-J.; Kim, C.-W. Reliability-Based Robust Design Optimization for Maximizing the Output Torque of Brushless Direct Current (BLDC) Motors Considering Manufacturing Uncertainty. *Machines* **2022**, *10*, 797. <https://doi.org/10.3390/machines10090797>

Academic Editors: Sven Matthiesen and Thomas Gwosch

Received: 18 August 2022

Accepted: 9 September 2022

Published: 10 September 2022

**Publisher's Note:** MDPI stays neutral with regard to jurisdictional claims in published maps and institutional affiliations.



**Copyright:** © 2022 by the authors. Licensee MDPI, Basel, Switzerland. This article is an open access article distributed under the terms and conditions of the Creative Commons Attribution (CC BY) license (<https://creativecommons.org/licenses/by/4.0/>).

**Keywords:** brushless direct current motor; manufacturing uncertainty; reliability-based robust design optimization; output torque; torque ripple; vibration analysis

## 1. Introduction

Electric motors are power-generating devices used in various industries, such as the automobile, home appliance, and plant industries. With the recent strengthening of environmental regulations worldwide, the application field of electric motors has expanded, and accordingly, designs with high energy density (through high output and miniaturization) and weight reduction have been developed. However, an increase in energy density causes an increase in torque ripple, which is one of the primary causes of electric motor vibration. Therefore, it is necessary to study the design of electric motors with high energy density while considering torque ripple.

Many studies have been conducted using the finite element analysis (FEA) method to analyze the vibration characteristics of electric motors and to reduce vibrations. R. Islam et al. analyzed the torque waveform and cogging torque according to the permanent magnet shape of a permanent-magnet synchronous motor (PMSM) using a two-dimensional

(2-D) electromagnetic (EM) FEA. They applied a step-skew type motor to reduce cogging torque [1]. C. Studer et al. explained the principle of cogging torque generation in electric motors using 2-D EM FEA and presented a method for reducing cogging torque using design variables, such as stator tooth and permanent magnet shape [2]. M. Dai et al. calculated the torque ripple of a permanent-magnet brushless direct current (BLDC) motor using 2-D EM FEA. They reduced the torque ripple by adjusting the skew angle [3]. J. Hong et al. analyzed the EM force using three-dimensional (3-D) EM FEA and proposed a design to reduce the vibration caused by EM force by changing the stator pole and yoke shape of a switched reluctance motor (SRM) [4].

With the improvement of analysis technology and computing power, several studies have been conducted to improve the performance of electric motors by applying various optimization methods. Previously, studies using the deterministic design optimization (DDO) method were conducted to reduce torque ripple. Choi et al. conducted a DDO study to minimize torque ripple using the air gap shape of an SRM as a design variable [5]. Kim et al. conducted a DDO study for maximizing the output torque using the permanent magnet volume of the spoke-type BLDC motor as a design variable [6]. Vasilija conducted a DDO study using the genetic algorithm with the rotor shape as a design variable to minimize the cogging torque of the PMSM [7]. Lee et al. conducted a multi-objective optimization study for maximizing output torque and minimizing torque ripple of SRM using the stator and rotor shapes as design variables [8,9]. Kuci et al. conducted a topology optimization study to minimize the torque ripple of the PMSM using the rotor shape [10]. Choi et al. conducted a DDO study to effectively obtain a sinusoidal distribution of the air gap flux density of IPM using the permanent magnet shape [11]. Consequently, it was possible to improve the output and vibration performance of the motor. However, since the DDO method is designed by setting the design variable to a single fixed value, it cannot consider the characteristics of fluctuations in product performance due to the uncertainty that occurs in the manufacturing process.

Mass production often results in performance variations due to uncertainties arising during the manufacturing process. Uncertainties are generally caused by production and assembly tolerances, material properties, and the environments of use [12]. Variations in performance due to uncertainty cause product failures. Considering the uncertainties that occur during mass production, the need for research on probabilistic design optimization (PDO) has emerged to achieve product performance and quality standards [13]. Depending on the purpose, PDO can be classified into robust design optimization (RDO) and reliability-based design optimization (RBDO) methods. RDO is a method used to minimize fluctuations in product performance and quality [14], and RBDO is a method used to increase product reliability at a given probability level [15]. In recent years, many studies have been conducted to design a motor using the above two methods.

Kim et al. performed an RDO study to improve the robustness of the cogging torque of BLDC motors and to improve the vibration performance [16]. Lee et al. conducted an RDO study using the stator and rotor shapes and rotor eccentricity as design variables to reduce the back electromotive force of the interior permanent-magnet synchronous motor (IPMSM) [17]. Lee et al. performed the design experiments to determine the design factors affecting the cogging torque of a surface-mounted permanent-magnet synchronous motor (SPMSM). They conducted an RDO study to reduce the cogging torque in consideration of the uncertainty that occurs during the assembly process of the stator [18]. Kim et al. conducted an RDO study to reduce the cogging torque of SPMSM by setting the uncertainty through FEA and experiments [19]. Consequently, it was possible to design a motor that simultaneously improves motor performance and minimizes quality fluctuations. Ziyang et al. performed RBDO to reduce the cogging torque considering the magnetic flux density of the stator [20]. Mun et al. performed RBDO to reduce the cogging torque by considering the performance variation due to manufacturing tolerance and operating temperature [21].

Reliability-based robust design optimization (RBRDO), which integrates RDO and RBDO, is the only way to consider both product quality and reliability in the design stage. Jang et al. performed RBRDO considering the manufacturing uncertainty of SPMSM. They proposed a design that minimizes the back electromotive force and increases the reliability of cogging torque [12]. Kim et al. conducted an RBRDO study of BLDC motors and reduced the cogging torque and the failure rate of output torque [22]. Hao et al. calculated the uncertainty using Monte Carlo simulation and performed RBRDO to minimize the mass of solid rocket motors [23]. Jang et al. performed RBRDO of IPMSM considering manufacturing and material uncertainty. They proposed a design to reduce torque ripple and the failure rate of output torque, and they explained the superiority of RBRDO by comparing the results of RBRDO, DDO, and RBDO [24]. The above studies tried to reduce torque ripple or cogging torque through EM design changes to improve vibration performance. However, the change in vibration response after design optimization was not analyzed.

In this study, considering the uncertainty caused by the manufacturing tolerances of BLDC motors, we proposed RBRDO as a multi-objective optimization that simultaneously maximizes the output torque and minimizes its standard deviation. We performed the EM–structural coupled analysis to calculate the output torque, torque ripple, and vibration response of the BLDC motor. To perform RBRDO, we selected the tooth thickness, slot opening (SO) width, slot radius, slot depth, tooth width, magnet thickness, and magnet length as the design variables related to the shape of the stator and rotor that affect the output torque of the motor. We performed the reliability analysis of the BLDC motor considering the distribution of the design variables. We used the rate of change compared to the initial value of the torque ripple and the area of the permanent magnet as constraints. We verified the superiority of RBRDO by comparing the results of RBRDO with those of DDO and RDO. Further, we performed a vibration analysis to analyze the change in vibration response in RBRDO compared to the initial BLDC motor.

## 2. Electromagnetic–Structural Coupled Analysis

We used the EM–structural coupled analysis to calculate the vibration response of a BLDC motor. We calculated the EM force acting on the stator tooth through the EM FEA. By applying the calculated EM force as the load condition of the structural finite element model, we calculated the acceleration response of the motor due to the EM force. In this study, we neglected the tangential EM force. The tangential EM force is generally negligible because its effect on the motor vibration is less than the radial EM force [25].

In this study, we used a BLDC motor with a rated output of 1.5 kW, 4 poles, and 24 slots, as shown in Figure 1. Table 1 summarizes the specifications of the BLDC motor.



Figure 1. BLDC motor.

**Table 1.** Specifications of the BLDC motor.

Specifications	Quantity
Type	BLDC
Number of poles	4
Number of slots	24
Rated power	1.5 kW
Rated torque	7.17 N·m
Rated speed	2000 rpm

The EM forces generated in the air gap cause the EM vibration of an electric motor. Using the principle of virtual work, we can calculate the EM force as follows:

$$\frac{\partial}{\partial s} \int_{\Omega} \int_0^H B \cdot dH d\Omega = F_s, \quad (1)$$

where  $B$  is the magnetic flux density,  $H$  is the magnetic field,  $s$  is the  $x$ ,  $y$ , and  $z$  axes in the Cartesian coordinate system, and  $\Omega$  is the domain where the nodal force  $F_s$  is applied. Applying Equation (1) to the mesh element  $e$  gives the following equation:

$$\int_e \left( -B^T \cdot J^{-1} \cdot \frac{\partial J}{\partial s} \cdot H + \int_0^H B \cdot dH \left| J^{-1} \right| \frac{\partial |J|}{\partial s} \right) dV = F_s, \quad (2)$$

where  $J$  is the Jacobian matrix of  $e$ , and  $V$  is the total volume. The Jacobian matrix is determined according to the element type. In the linear case, the integral of  $B$  can be simplified as follows:

$$\int_0^H B \cdot dH = \int_0^H \mu H \cdot dH = \frac{\mu}{2} |H|^2, \quad (3)$$

where  $\mu$  is the magnetic relative permeability. Using (1), (2), and (3), the local force  $F_s^i$  applied to a given node  $i$  can be formulated as follows:

$$\sum_{\forall e} \int_e \left( -B^T \cdot J^{-1} \cdot \frac{\partial J}{\partial s} \cdot H + \frac{\mu}{2} |H|^2 \left| J^{-1} \right| \frac{\partial |J|}{\partial s} \right) dV = F_s^i. \quad (4)$$

Equation (4) can be expressed in the matrix form as follows:

$$- [\mathbf{B}]^T [\mathbf{J}]^{-1} [\mathbf{H}] \nabla J + \frac{\mu}{2} [\mathbf{H}]^2 [\mathbf{J}]^{-1} \nabla J = \{F_s\}. \quad (5)$$

We performed an EM analysis using the 2-D cross-sectional model shown in Figure 2 to calculate the output torque, torque ripple, and EM force acting on the stator tooth of the BLDC motor. A three-phase alternating current at 2000 rpm rated operation was applied as the analysis condition.

As a result of the EM analysis, the output torque and torque ripple were calculated as 7.16 N·m and 3.46 N·m, respectively, as shown in Figure 3. Compared with the performance specification of the BLDC motor (7.17 N·m), the relative error is 0.14%.

The radial EM force acting on the stator tooth was calculated as shown in Figure 4. Vibration analysis was performed by inputting the calculated radial EM force into the stator structure.

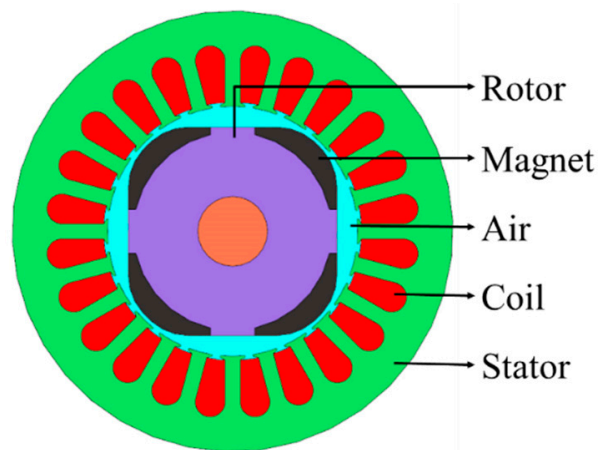


**Figure 2.** 2-D cross-section of the BLDC motor.

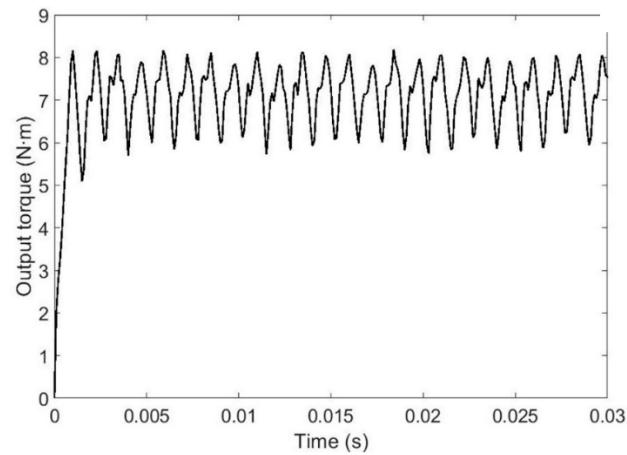


**Figure 3.** Output torque of the BLDC motor.

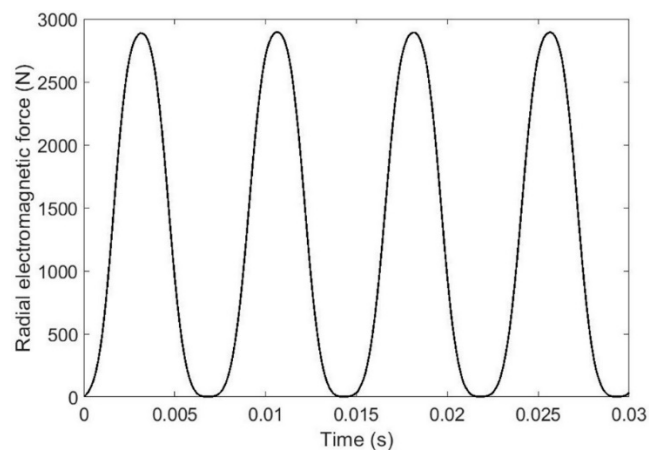


**Figure 4.** Radial EM force acting on a single stator tooth.

The mechanical properties of BLDC motors can be described using the following equation of motion:

$$[\mathbf{M}]\{\ddot{x}\} + [\mathbf{C}]\{\dot{x}\} + [\mathbf{K}]\{x\} = \{F(t)\}, \quad (6)$$

where  $[\mathbf{M}]$ ,  $[\mathbf{C}]$ , and  $[\mathbf{K}]$  represent a mass matrix, damping matrix, and stiffness matrix, respectively.  $\{x\}$  is the displacement vector and  $\{F(t)\}$  is the applied load vector.

The harmonic components of the EM force calculated through the EM analysis were applied to the stator tooth of the 3-D finite element model. Transient analysis using the EM-

structural coupled analysis method was performed to calculate the acceleration response in the finite element model of the BLDC motor shown in Figure 5. Fast Fourier transform was performed to obtain the normalized frequency response curve shown in Figure 6.

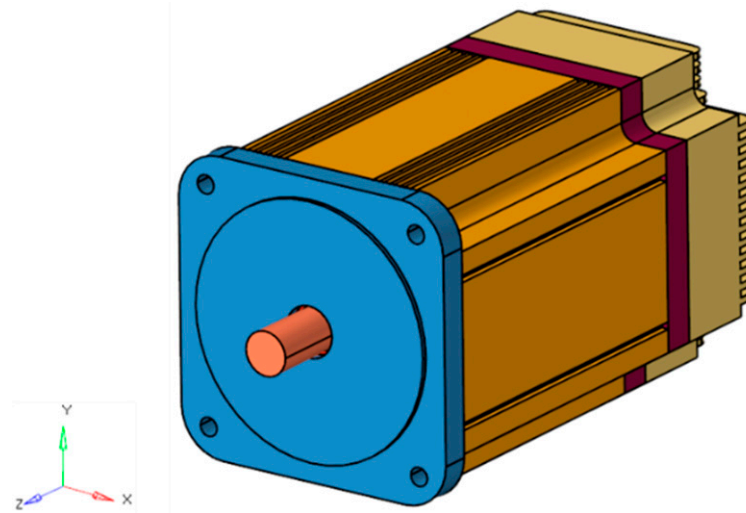


**Figure 5.** Finite element model of the BLDC motor.

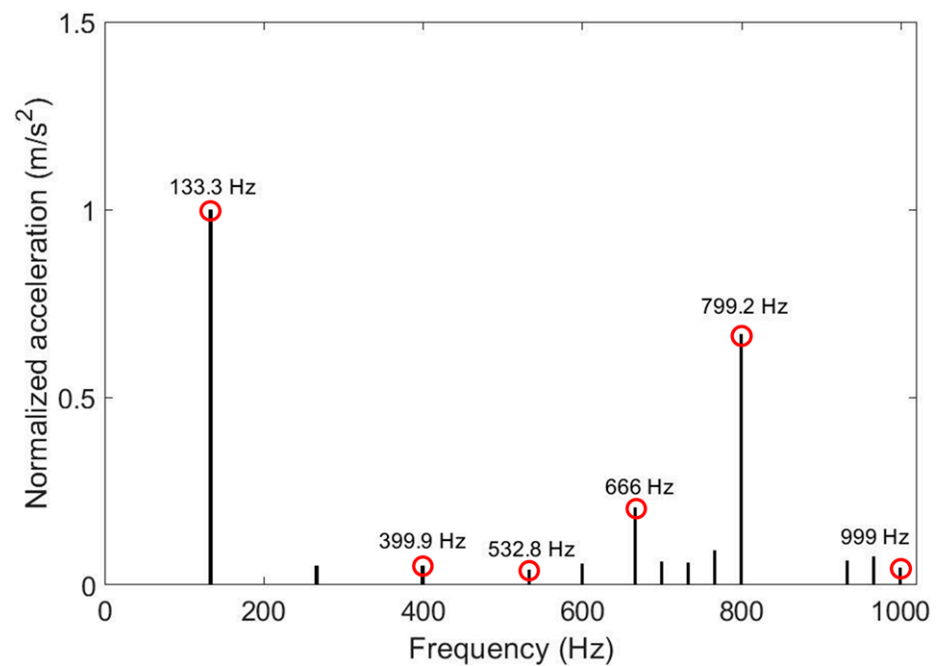


**Figure 6.** Normalized acceleration and peak frequencies of the finite element BLDC motor model.

The vibration measurement data in Figure 7 were used to verify the EM–structural coupled analysis results [26]. Table 2 summarizes the relative errors of the peak frequencies of the EM–structural coupled analysis and the vibration measurement results. The maximum relative error of the analysis and experiment for the frequency at which the peak acceleration value occurs in the range of 0 to 1000 Hz is less than 4%. We verified the vibration prediction accuracy of the analysis model. The reason for the difference of 133.3 Hz in the magnitude of the analysis and measurement results is that a sinusoidal current without harmonic components was applied to the input current. We performed a reliability analysis and RBRDO of the BLDC motor using the verified analysis model.



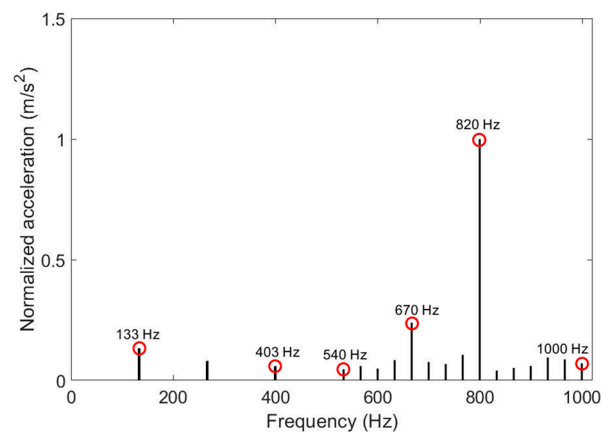


**Figure 7.** Normalized acceleration and peak frequencies of the measured point.

**Table 2.** Comparison of the peak frequencies of measured and simulated results.

Measured Peak Frequency (Hz)	Simulated Peak Frequency (Hz)	Relative Error (%)
133	133.3	0.23%
276	266.6	−3.48%
403	399.9	−0.77%
540	532.8	−1.33%
612	599.4	−2.06%
670	666	−0.60%
705	699.3	−0.81%
724	732.6	1.19%
780	765.9	−1.81%
820	799.2	−2.54%
943	932.4	−1.12%
986	965.7	−2.06%
1000	999	−0.10%

### 3. Probabilistic Design Optimization

The design optimization method is divided into DDO and PDO depending on whether the uncertainty of the design variables is considered. DDO is a traditional design optimization method in which the design variables are assumed to have a fixed value without considering uncertainty.

The DDO problem can be formulated as follows:

$$\begin{aligned} & \min f(\mathbf{d}), \\ & \text{subject to } g_i(\mathbf{d}) < 0, i = 1, 2, \dots, \end{aligned} \quad (7)$$

where  $f$  is the objective function for the design variable  $\mathbf{d}$ , and  $g$  is the constraint.

Because DDO does not consider the uncertainty of design variables, the product performance may vary, thereby not satisfying the requirements of the designer or causing product failures. Therefore, a PDO method that considers the uncertainty of design variables was used. PDO can be divided into RBDO and RDO depending on whether the design purpose is to satisfy the reliability or minimize the performance fluctuation.

RBDO is used to design a product that satisfies the reliability as per the requirement of the designer by quantitatively defining uncertainty. Therefore, reliability analysis is necessary to accurately predict the failure probability of a constraint condition. Reliability is a design condition in product design that refers to satisfying the required performance. The design variable is defined as a probability variable  $X$  to consider reliability quantitatively. A performance function representing the required performance is defined as  $g$  to evaluate the reliability of a product. As shown in Figure 8, the performance function is expressed as

a probability density function, and at the performance function equals 0, it is divided into a feasible and an infeasible region that satisfies the constraint condition. The probability of product damage is obtained by calculating the area where  $g > 0$  in the probability density function curve shown in Figure 8. Reliability increases as the probability of damage decreases [27].

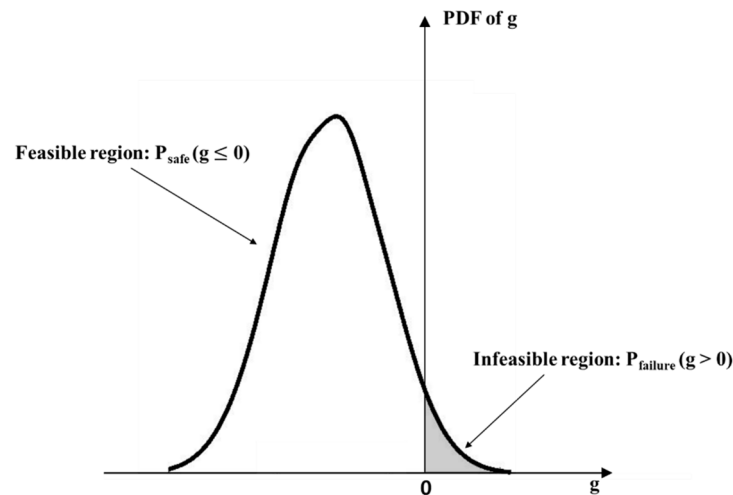


**Figure 8.** Probability density function of a performance function.

The RBDO problem can be formulated as follows:

$$\begin{aligned} & \min h(\mathbf{d}), \\ & \text{subject to } P_F(g_i(\mathbf{X}) > 0) \geq P_{t,i}, i = 1, 2, \dots, \end{aligned} \quad (8)$$

where  $h$  is the objective function,  $g_i$  is the  $i$ -th constraint function,  $P_F$  is the failure rate under infeasible conditions, and  $P_{t,i}$  is the  $i$ -th target value to guarantee the reliability of  $g_i$ .

Robust design is a method that additionally considers robustness in the existing design method and was first developed by Taguchi Genichi. The Taguchi method uses the S/N ratio and orthogonal array as evaluation indices for robustness to minimize the performance fluctuations due to noise factors [28,29]. The Taguchi method maximizes the S/N ratio to reduce the variation of the quality loss function and further uses an adjustment parameter such that the average of the quality loss function reaches the target value. Through this process, we can discover a design that reduces the fluctuation of the quality loss function and simultaneously satisfies the target performance.

However, since robust design uses an orthogonal arrangement table, it is difficult to consider a wide design range, and the design variables can be defined only in a discrete space. In addition, the general design requires many constraint conditions. The Taguchi method is inefficient in dealing with these constraints. RDO, a mathematically well-developed design optimization method, is used to solve the above problems [30].

RDO is used to find a design in which the product performance is insensitive to uncertainties, such as the variations of design variables. In this method, the mean of the quality loss function is optimized, and the variance is minimized while satisfying the design constraints. The RDO problem can be formulated as follows:

$$\begin{aligned} & \min f(\mu_h, \sigma_h^2), h(\mathbf{X}; \mathbf{d}), \\ & \text{subject to } g_i(\mathbf{d}) \leq 0, i = 1, 2, \dots, \end{aligned} \quad (9)$$

where  $f$  is the quality loss function consisting of mean  $\mu_h$  and variance  $\sigma_h^2$  for  $h$ . Since  $f$  is expressed as the sum of the mean and variance multiplied by a specific weight, RDO is a multi-objective optimization.  $\mathbf{d}$  is a vector of design variables defined as  $\mathbf{d} = \mu(\mathbf{X})$ , where



$\mu$  represents the mean of the design probability variable  $X$ . The purpose of RDO is to find the design that is most insensitive to changes in probability variables within the effective design domain  $g_i \leq 0$  [28].

RBRDO is a method that integrates the above two design optimization methods to minimize the performance fluctuation characteristics and simultaneously satisfy the reliability level required by the designer. In the problem formulation of RBRDO, the loss function of the product quality is minimized according to the probabilistic constraint shown in the following equation:

$$\begin{aligned} & \min f(\mu_h, \sigma_h^2), h(\mathbf{X}; \mathbf{d}), \\ & \text{subject to } P_F(g_i(\mathbf{X}) > 0) \geq P_{t,i}, i = 1, 2, \dots \end{aligned} \quad (10)$$

RDO and RBDO are integrated into one numerical model to solve Equation (10). Although such an integrated optimization problem requires a high computational cost, it has an increasing need because it enables a robust and reliable product design against changes in design variables.

#### 4. Reliability-Based Robust Design Optimization of the BLDC Motor

##### 4.1. Reliability Analysis of the BLDC Motor

The stator and rotor of the BLDC motor are generally manufactured through the stamping process. There are uncertainties in the manufacturing process due to various factors, such as manufacturing tolerances and assembly environment. These uncertainties can eventually lead to variations in motor performance. The performance variation of the motor may not satisfy the requirements of the designer and may increase the failure rate. Therefore, we require a design considering the uncertainty caused by the manufacturing tolerance of the BLDC motor.

The design variables that affect the motor's output performance are defined as shown in Figure 9. Table 3 summarizes the distribution of design variables caused by the uncertainty of manufacturing tolerances during the stamping process. In this study, we referred to the stamping uncertainty of the metal plate proposed in [31]. Baron et al. recommended a standard deviation of 0.06 mm for the stamping process. We performed a reliability analysis to calculate the performance variation of the BLDC motor. Table 4 summarizes the reliability analysis results. Figure 10 shows the probability distributions for the output torque and torque ripple of BLDC motors.

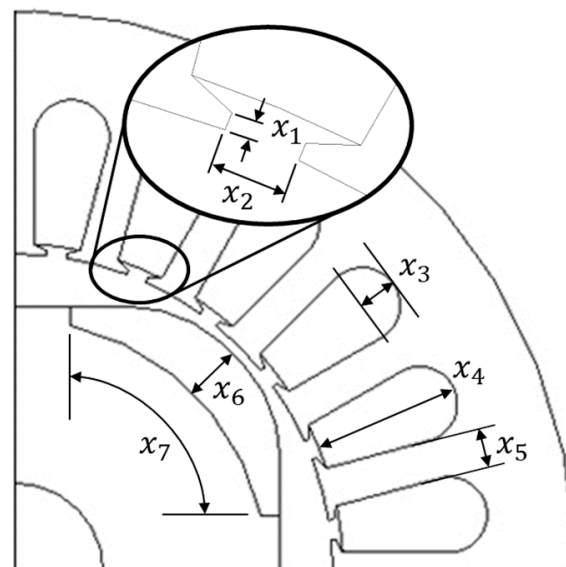


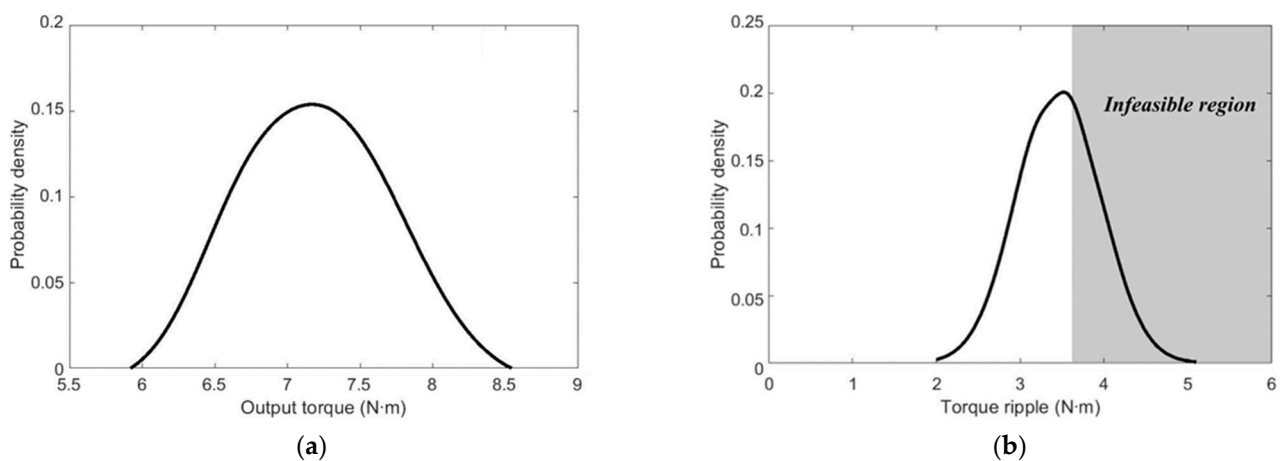
Figure 9. Design variables of the BLDC motor.

**Table 3.** Probabilistic distribution of the design variables of the BLDC motor.

Parameters	Unit	Mean	Standard Deviation	Distribution
Tooth thickness $x_1$	mm	0.5	0.06	Normal
SO width $x_2$	mm	2.18	0.06	Normal
Slot radius $x_3$	mm	4.05	0.06	Normal
Slot depth $x_4$	mm	15.86	0.06	Normal
Tooth width $x_5$	mm	4.19	0.06	Normal
Magnet thickness $x_6$	mm	6	0.06	Normal
Magnet length $x_7$	mm	37.53	0.06	Normal

**Table 4.** Reliability analysis of the BLDC motor.

Output torque	Mean (N·m)	7.16
	Standard deviation	0.49
Torque ripple	Mean (N·m)	3.46
	Probability of failure (%)	36.81

**Figure 10.** Probability distributions of (a) output torque and (b) torque ripple of the BLDC motor.

#### 4.2. Design Optimization for Maximizing the Output Torque of the BLDC Motor

We applied various optimization methods to improve the output torque of the BLDC motor. We performed a DDO that does not consider the distribution of design variables due to the manufacturing uncertainty of BLDC motors. However, DDO has a limit in reducing the performance variation when considering the distribution of each variable. An RDO, which can minimize performance variation, was performed to overcome the limitations of DDO. Finally, we performed RBRDO to reduce performance variation and failure rate simultaneously. Table 5 summarizes the design variables and spaces of BLDC motors.

The purpose of the DDO of the BLDC motor is to maximize the output torque. The constraint conditions of DDO are torque ripple and magnet area, and the change is limited to +5% of the initial value. Equation (11) shows the formulation of the DDO of the BLDC motor.

$$\begin{aligned}
 & \text{Find } x_i (i = 1, \dots, 7), \\
 & \text{Maximize } T_{out}(x_i), \\
 & \text{Subject to } g_1(x_i) \leq 1.05 T_{ripp,initial}, \\
 & \quad \quad g_2(x_i) \leq 1.05 A_{initial}.
 \end{aligned} \tag{11}$$

$x_i$  represents the seven design variables that determine the shape of the motor,  $T_{out}$  is a function of output torque, and  $g_1$  and  $g_2$  represent the functions of torque ripple and magnet area, respectively.

**Table 5.** Design variables and their bounds.

Design Variables	Unit	Design Spaces
Tooth thickness $x_1$	mm	$0.2 < x_1 < 0.98$
SO width $x_2$	mm	$1.96 < x_2 < 2.39$
Slot radius $x_3$	mm	$3.65 < x_3 < 4.45$
Slot depth $x_4$	mm	$11.19 < x_4 < 20.56$
Tooth width $x_5$	mm	$3.69 < x_5 < 4.68$
Magnet thickness $x_6$	mm	$3.45 < x_6 < 8.35$
Magnet length $x_7$	mm	$35.53 < x_7 < 39.53$

RDO of the BLDC motor is a multi-objective optimization that can minimize performance variation while maximizing performance by considering the distribution of design variables due to manufacturing uncertainty. The first and second objective functions are the maximization and minimization of the mean value of the output torque, respectively. The constraint conditions are the same as the formulation of the DDO. Equation (12) shows the RDO problem formulation.

$$\begin{aligned}
 & \text{Find } x_i (i = 1, \dots, 7), \\
 & \text{Maximize } F = \left( w_1 \frac{\mu_f}{\mu_{f0}} + w_2 \frac{\sigma_{f0}}{\sigma_f} \right), \\
 & \text{Subject to } g_1(x_i) \leq 1.05 T_{ripp,initial}, \\
 & \quad \quad \quad g_2(x_i) \leq 1.05 A_{initial}.
 \end{aligned} \tag{12}$$

$F$ ,  $\mu_f$ , and  $\sigma_f$  represent the mean and standard deviation, mean value, and standard deviation of the output torque, respectively.  $\mu_{f0}$  and  $\sigma_{f0}$  are initial values of the mean and standard deviation of the output torque, respectively.  $w_1$  and  $w_2$  are weight factors of 0.5 and 1, respectively.

Equation (13) is the formula for the problem of RBRDO, which increases the robustness of the performance and reduces the failure rate by considering the manufacturing uncertainty of the BLDC motor. Figure 11 shows the RBRDO flowchart. The objective function is the same as the formulation of the RDO. The constraint condition is the failure rate; 99% reliability is achieved within the +5% change rate compared to the initial torque ripple. In this study, we used the system reliability optimization method for the RBRDO of the BLDC motor. This method is suitable when there are various constraints [32].

$$\begin{aligned}
 & \text{Find } x_i (i = 1, \dots, 7), \\
 & \text{Maximize } F = \left( w_1 \frac{\mu_f}{\mu_{f0}} + w_2 \frac{\sigma_{f0}}{\sigma_f} \right), \\
 & \text{Subject to } Pr \left( g_1(x_i) \leq 1.05 T_{ripp,initial} \right) \geq 0.99, \\
 & \quad \quad \quad g_2(x_i) \leq 1.05 A_{initial}.
 \end{aligned} \tag{13}$$

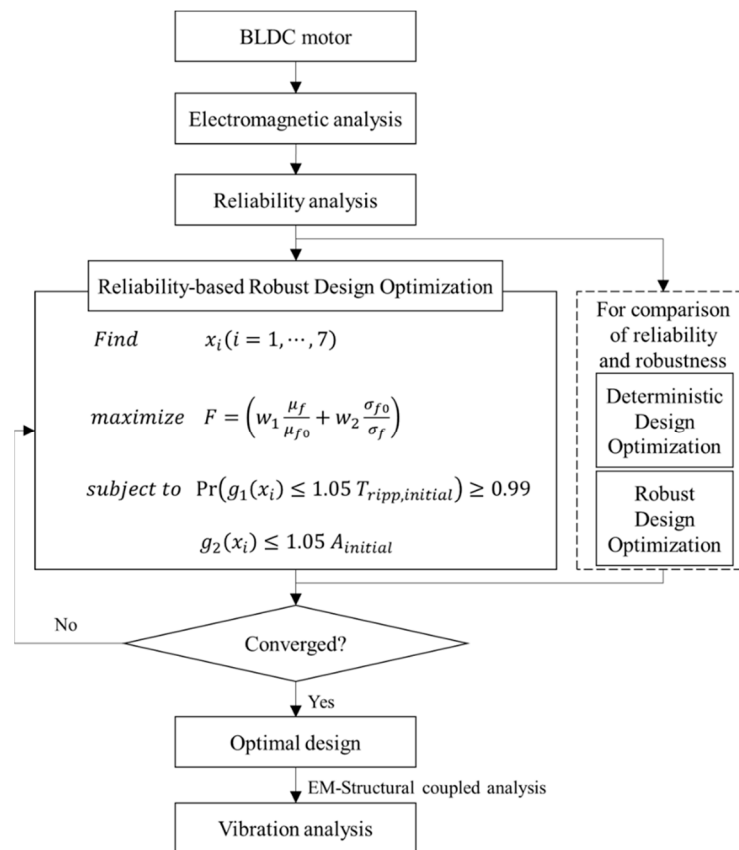


**Figure 11.** Flowchart of the RBRDO method.

## 5. Results and Discussion

### 5.1. RBRDO Results

Table 6 shows the changes in design variables and performance before and after RBRDO. Figure 12 shows the superiority of RBRDO by comparing the probability distribution results of the output torque and torque ripple of the initial BLDC motor and RBRDO. Consequently, the mean value of the output torque increased by 9% compared to the initial design to 7.79 N·m. The standard deviation of the output torque decreased by 45.8% compared to the initial design to 0.26, resulting in a robust design. The mean value of torque ripple decreased by 51.7% compared to the initial design to 1.67 N·m. The failure rate decreased by 99.2% compared to the initial design to 0.28%. The magnet area was 151.1 mm<sup>2</sup>, which satisfied the constraint condition.

**Table 6.** Comparison of the design variables and performances in the initial design and RBRDO.

Design Variables and Performance		Initial Design	RBRDO	Rate of Change (%)
	Tooth thickness (mm)	0.5	0.46	−8.0
	SO width (mm)	2.18	2.37	+8.7
	Slot radius (mm)	4.05	3.78	−6.7
	Slot depth (mm)	15.86	11.2	−29.5
	Tooth width (mm)	4.19	3.70	−11.9
	Magnet thickness (mm)	6	5	−16.7
	Magnet length (mm)	37.53	39.52	+5.3
Output torque	Mean (N·m)	7.16	7.79	+8.8
	Standard deviation	0.49	0.26	−46.9
Torque ripple	Mean (N·m)	3.46	1.67	−51.7
	Probability of failure (%)	36.8	0.28	−99.2
	Magnet area (mm <sup>2</sup> )	152.5	151.1	−0.92

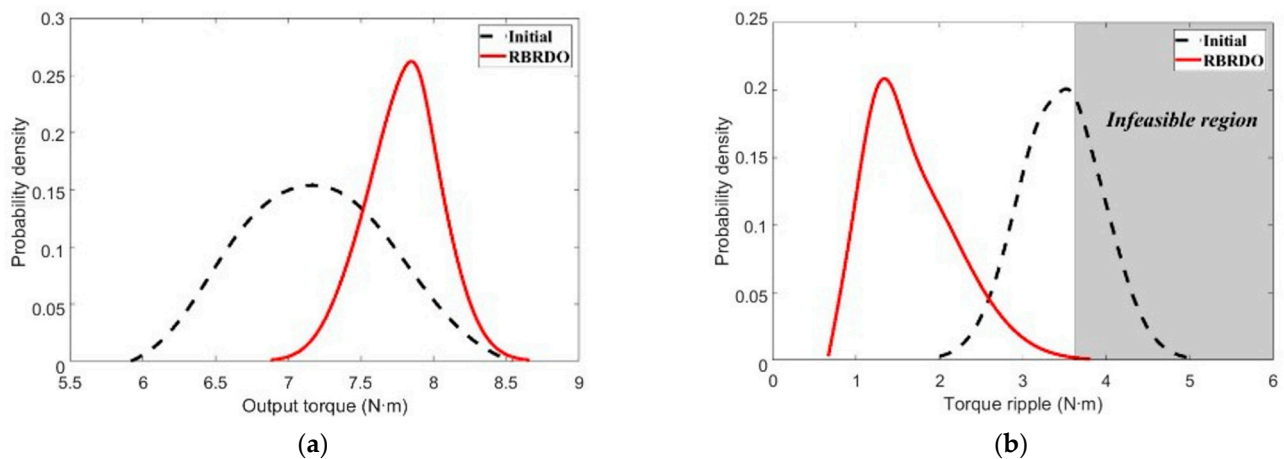


**Figure 12.** Comparison of probability distribution results of (a) output torque and (b) torque ripple in the initial design and RBRDO.

### 5.2. Comparison of Results of RBRDO with Those of DDO and RDO

In this study, we performed RBRDO to maximize the output torque and reduce the performance variation and failure rate simultaneously, considering the manufacturing uncertainty of the BLDC motor. We compared the design optimization results of RBRDO with those of the DDO and RDO methods to confirm that RBRDO provides better reliability and robustness than DDO or RDO. Compared to DDO, RBRDO considers uncertainty. Thus, it minimizes the standard deviation of performance to improve robustness. In addition, RBRDO can reduce the failure rate by improving reliability.

Table 7 summarizes each optimization result's output torque, torque ripple, and failure rate. Figure 13 shows the probability distributions of output torque and torque ripple as the result of reliability analysis for each optimization method. In the case of DDO, the average output torque was 8.49 N·m, and the optimal solution with the highest value was derived. However, considering the distribution of design variables, the standard deviation of the output torque was 0.54, which cannot reduce the performance variation that occurs during mass production. The torque ripple failure rate was 33.0%. In the case of RDO, the mean value of the output torque was 8.29 N·m, and the standard deviation was reduced by 50% compared to DDO, resulting in a robust design for output performance. However, the failure rate of 10.1% occurred because the constraint condition for the failure rate was not considered. In the case of RBRDO, the mean value of output torque was 7.79 N·m, and the standard deviation was 0.26. Compared to the initial design, it was possible to increase the output torque and reduce the variation of output performance. In addition, the torque ripple was 1.67 N·m, and the failure rate was the lowest at 0.28%.

**Table 7.** Comparison of DDO, RDO, and RBRDO results.

		Optimization Method		
		DDO	RDO	RBRDO
Output torque (N·m)	Mean	8.49	8.28	7.79
	Standard deviation	0.54	0.24	0.26
Torque ripple (N·m)	Mean	3.35	2.63	1.67
	Probability of failure (%)	33.0	10.1	0.28
Magnet area (mm <sup>2</sup> )		160.0	153.2	151.1

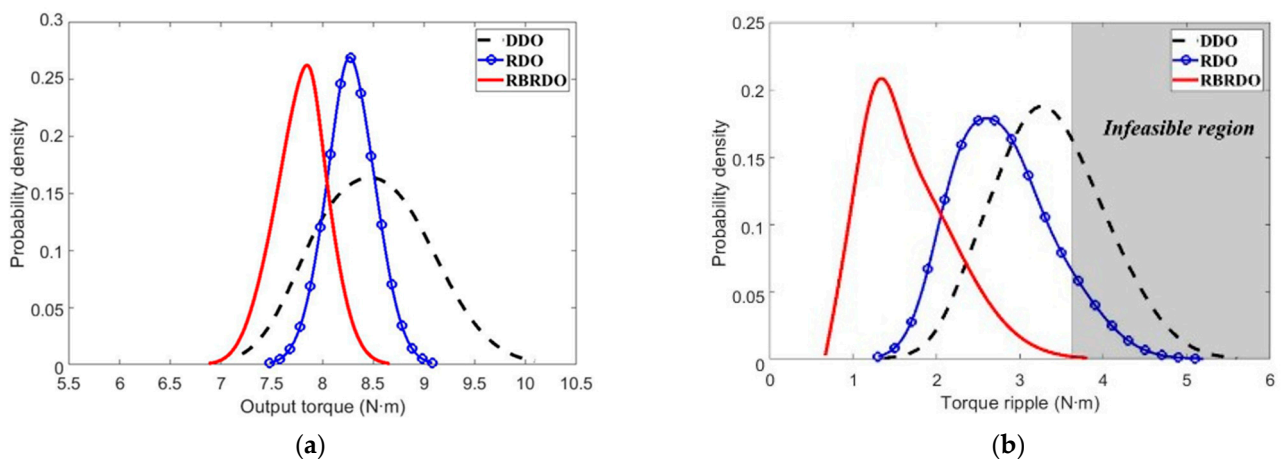


**Figure 13.** Comparison of DDO, RDO, and RBRDO results for (a) output torque and (b) torque ripple.

To compare the vibration responses of the initial BLDC motor and RBRDO model, EM–structural coupled analysis was performed. Figure 14 shows the frequency response graph of the vibration analysis results. It is a response to the EM force. The fundamental frequency of 133.3 Hz increased by 9% from  $2.18 \text{ m/s}^2$  to  $2.38 \text{ m/s}^2$  due to the energy density increase. However, the response at 400 Hz and the frequency component of torque ripple decreased (by 18.2%) from  $0.11 \text{ m/s}^2$  to  $0.09 \text{ m/s}^2$ . We used the root mean square (RMS) method to compare the magnitude of the vibration response from 0 to 1000 Hz. The RMS value of the vibration response of the initial BLDC motor was 0.748. The RMS value of the vibration response of the RBRDO model increased by 2% to 0.763. However, since the output torque increased by 9% with RBRDO, we could confirm that a higher increase is possible in the output torque than the magnitude of the vibration response.

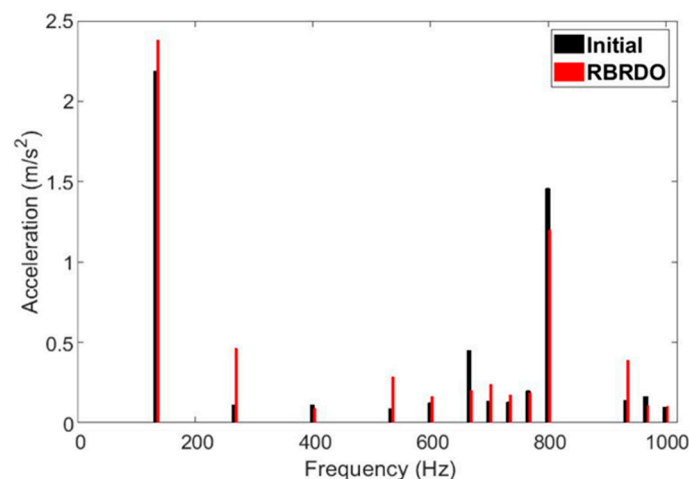


**Figure 14.** Comparison of vibration analysis results of initial BLDC motor and RBRDO.

## 6. Conclusions

In this paper, we proposed RBRDO to improve the output torque of the BLDC motor and simultaneously reduce the failure rate and output torque standard deviation caused by uncertainty due to manufacturing tolerance. Using the EM–structural coupled analysis, we calculated the output torque and torque ripple, when the BLDC motor rotated at the rated speed, and analyzed the vibration characteristics. We selected the tooth thickness, SO width, slot radius, slot depth, tooth width, magnet thickness, and magnet length as the design variables related to the shape of the stator and rotor, which affected the motor's output performance, to perform RBRDO. We performed a reliability analysis of the BLDC motor using the output torque and torque ripple calculated through EM analysis. We



defined RBRDO as a multi-objective function to maximize the output torque and minimize the standard deviation of the output torque. We set the constraint condition to have a reliability of 99% within a rate of change of +5% compared to the initial torque ripple.

As a result of RBRDO, the optimal design of the mean value of output torque was 7.79 N·m, which increased by 8.8% compared to the initial BLDC motor, and the standard deviation decreased (by 46.9%) to 0.26. The mean value of torque ripple was reduced by 51.7% compared to the initial design to 1.67 N·m, and the failure rate decreased by 99.2%. We performed DDO and RDO to confirm that RBRDO showed better robustness and reliability, and all results were compared through reliability analysis considering the distribution of design variables. Comparing the results of RBRDO and DDO, we confirmed that the standard deviation of the output torque, which indicates the performance variation of the motor, was reduced by 51.9% through the improvement of robustness. Using RBRDO, the failure rate decreased by 97.2% through improved reliability. Therefore, the RBRDO of the BLDC motor maximizes the output torque while reducing failure rate and performance variation caused by manufacturing uncertainty. In addition, comparing the vibration response of the initial BLDC motor and the RBRDO model revealed that when the output torque increased by 9%, the vibration response increased by 2%; this confirmed that RBRDO could increase the energy density without affecting the vibration response.

The proposed procedure proved to be an effective design method for improving the output performance of a motor while considering both reliability and robustness. However, additional research should be conducted on the multi-objective reliability-based robust design optimization to reduce vibration while improving the output performance of the motor. The multi-objective reliability-based robust design optimization increases the computational cost exponentially. As a future work, the authors intend to develop a new solution for a multi-purpose, reliability-based robust design for improving the output performance of the motor and reducing vibration while considering the computational cost.

**Author Contributions:** Conceptualization, K.J. and C.-W.K.; Methodology, K.J. and C.-W.K.; Software, K.J.; Validation, K.J. and C.-W.K.; Formal Analysis, K.J. and D.Y.; Investigation, K.J.; Resources, K.J.; Data Curation, K.J.; Writing—Original Draft Preparation, K.J.; Writing, Review, and Editing, K.J., J.P. and C.-W.K.; Visualization, K.J.; Supervision, C.-W.K., J.-J.L. and K.-D.L.; Project Administration, C.-W.K.; Funding Acquisition, C.-W.K. All authors have read and agreed to the published version of the manuscript.

**Funding:** This paper was supported by Konkuk University Researcher Fund in 2021 and the Technology Innovation Program (20012518) funded By the Ministry of Trade, Industry and Energy (MOTIE, Korea).

**Institutional Review Board Statement:** Not applicable.

**Informed Consent Statement:** Not applicable.

**Data Availability Statement:** Not applicable.

**Conflicts of Interest:** The authors declare no conflict of interest.

## References

1. Islam, R.; Husain, I.; Fardoun, A.; McLaughlin, K. Permanent magnet synchronous motor magnet designs with skewing for torque ripple and cogging torque reduction. In Proceedings of the 2007 IEEE Industry Applications Annual Meeting, New Orleans, LA, USA, 23–27 September 2007; pp. 1552–1559.
2. Studer, C.; Keyhani, A.; Sebastian, T.; Murthy, S.K. Study of cogging torque in permanent magnet machines. In Proceedings of the IAS'97. Conference Record of the 1997 IEEE Industry Applications Conference Thirty-Second IAS Annual Meeting, New Orleans, LA, USA, 5–9 October 1997; pp. 42–49.
3. Dai, M.; Keyhani, A.; Sebastian, T. Torque ripple analysis of a PM brushless DC motor using finite element method. *IEEE Trans. Energy Convers.* **2004**, *19*, 40–45. [[CrossRef](#)]
4. Hong, J.P.; Ha, K.H.; Lee, J. Stator pole and yoke design for vibration reduction of switched reluctance motor. *IEEE Trans. Magn.* **2002**, *38*, 929–932. [[CrossRef](#)]
5. Choi, Y.K.; Yoon, H.S.; Koh, C.S. Pole-shape optimization of a switched-reluctance motor for torque ripple reduction. *IEEE Trans. Magn.* **2007**, *43*, 1797–1800. [[CrossRef](#)]

6. Kim, H.W.; Kim, K.T.; Jo, Y.S.; Hur, J. Optimization methods of torque density for developing the neodymium free SPOKE-type BLDC motor. *IEEE Trans. Magn.* **2013**, *49*, 2173–2176. [[CrossRef](#)]
7. Sarac, V. Performance optimization of permanent magnet synchronous motor by cogging torque reduction. *J. Electr. Eng.* **2019**, *70*, 218–226. [[CrossRef](#)]
8. Lee, C.; Lee, J.; Jang, I.G. Shape optimization-based design investigation of the switched reluctance motors regarding the target torque and current limitation. *Struct. Multidiscip. Optim.* **2021**, *64*, 859–870. [[CrossRef](#)]
9. Lee, C.; Jang, I.G. Topology optimization of multiple-barrier synchronous reluctance motors with initial random hollow circles. *Struct. Multidiscip. Optim.* **2021**, *64*, 2213–2224. [[CrossRef](#)]
10. Kuci, E.; Henrotte, F.; Duysinx, P.; Geuzaine, C. Combination of topology optimization and Lie derivative-based shape optimization for electro-mechanical design. *Struct. Multidiscip. Optim.* **2019**, *59*, 1723–1731. [[CrossRef](#)]
11. Choi, J.S.; Izui, K.; Nishiwaki, S.; Kawamoto, A.; Nomura, T. Rotor pole design of IPM motors for a sinusoidal air-gap flux density distribution. *Struct. Multidiscip. Optim.* **2012**, *46*, 445–455. [[CrossRef](#)]
12. Jang, J.; Cho, S.G.; Lee, S.J.; Kim, K.S.; Kim, J.M.; Hong, J.P.; Lee, T.H. Reliability-based robust design optimization with kernel density estimation for electric power steering motor considering manufacturing uncertainties. *IEEE Trans. Magn.* **2015**, *51*, 8001904. [[CrossRef](#)]
13. Kim, N.K.; Kim, D.H.; Kim, D.W.; Kim, H.G.; Lowther, D.A.; Sykulski, J.K. Robust optimization utilizing the second-order design sensitivity information. *IEEE Trans. Magn.* **2010**, *46*, 3117–3120. [[CrossRef](#)]
14. Park, G.J.; Lee, T.H.; Lee, K.H.; Hwang, K.H. Robust design: An overview. *AIAA J.* **2006**, *44*, 181–191. [[CrossRef](#)]
15. Youn, B.D.; Choi, K.K.; Du, L. Enriched Performance Measure Approach for Reliability-Based Design Optimization. *AIAA J.* **2005**, *43*, 874–884. [[CrossRef](#)]
16. Kim, D.W.; Choi, N.S.; Lee, C.U.; Kim, D.H. Assessment of statistical moments of a performance function for robust design of electromagnetic devices. *IEEE Trans. Magn.* **2015**, *51*, 7205104. [[CrossRef](#)]
17. Lee, S.J.; Kim, K.S.; Cho, S.G.; Jang, J.; Lee, T.; Hong, J.P. Taguchi robust design of back electromotive force considering the manufacturing tolerances in IPMSM. In Proceedings of the 2012 Sixth International Conference on Electromagnetic Field Problems and Applications, Dalian, China, 19–21 June 2012; pp. 1–4.
18. Lee, S.G.; Kim, S.; Park, J.C.; Park, M.R.; Lee, T.H.; Lim, M.S. Robust Design Optimization of SPMSM for Robotic Actuator Considering Assembly Imperfection of Segmented Stator Core. *IEEE Trans. Energy Convers.* **2020**, *35*, 2076–2085. [[CrossRef](#)]
19. Kim, S.; Lee, S.G.; Kim, J.M.; Lee, T.H.; Lim, M.S. Robust design optimization of surface-mounted permanent magnet synchronous motor using uncertainty characterization by bootstrap method. *IEEE Trans. Energy Convers.* **2020**, *35*, 2056–2065. [[CrossRef](#)]
20. Ren, Z.; Ma, J.; Qi, Y.; Zhang, D.; Koh, C.S. Managing Uncertainties of Permanent Magnet Synchronous Machine by Adaptive Kriging Assisted Weight Index Monte Carlo Simulation Method. *IEEE Trans. Energy Convers.* **2020**, *35*, 2162–2169. [[CrossRef](#)]
21. Mun, J.; Lim, J.; Kwak, Y.; Kang, B.; Choi, K.K.; Kim, D.H. Reliability-based design optimization of a permanent magnet motor under manufacturing tolerance and temperature fluctuation. *IEEE Trans. Magn.* **2021**, *57*, 8203304. [[CrossRef](#)]
22. Kim, D.W.; Kang, B.; Choi, K.K.; Kim, D.H. A comparative study on probabilistic optimization methods for electromagnetic design. *IEEE Trans. Magn.* **2015**, *52*, 7201304. [[CrossRef](#)]
23. Hao, Z.; Haowen, L.; Pengcheng, W.; Guobiao, C.; Feng, H. Uncertainty analysis and design optimization of solid rocket motors with finocyl grain. *Struct. Multidiscip. Optim.* **2020**, *62*, 3521–3537. [[CrossRef](#)]
24. Jang, G.U.; Kim, C.W.; Bae, D.; Cho, Y.; Lee, J.J.; Cho, S. Reliability-based robust design optimization for torque ripple reduction considering manufacturing uncertainty of interior permanent magnet synchronous motor. *J. Mech. Sci. Technol.* **2020**, *34*, 1249–1256. [[CrossRef](#)]
25. Gieras, J.F.; Wang, C.; Lai, J.C. *Noise of Polyphase Electric Motors*; CRC Press: Boca Raton, FL, USA, 2018.
26. Cho, S.; Hwang, J.; Kim, C.W. A study on vibration characteristics of brushless dc motor by electromagnetic-structural coupled analysis using entire finite element model. *IEEE Trans. Energy Convers.* **2018**, *33*, 1712–1718. [[CrossRef](#)]
27. Kang, B.; Choi, K.K.; Kim, D.H. An efficient serial-loop strategy for reliability-based robust optimization of electromagnetic design problems. *IEEE Trans. Magn.* **2017**, *54*, 7000904. [[CrossRef](#)]
28. Taguchi, G. *Introduction to Quality Engineering: Designing Quality into Products and Processes*; Asian Productivity Organization: Tokyo, Japan, 1986.
29. Taguchi, G. *System of Experimental Design; Engineering Methods to Optimize Quality and Minimize Costs*; UNIPUB/Kraus International Publications: White Plains, NY, USA, 1987.
30. Park, G.J. Design of experiments. In *Analytic Methods for Design Practice*; Springer: London, UK, 2007; pp. 309–391.
31. Baron, J.; Hammett, P.; Smith, D. *Stamping Process Variation: An Analysis of Stamping Process Capability and Implications for Design, Die Tryout and Process Control*; Technical Report Prepared for the Auto Steel Partnership Program: Southfield, MI, USA, 1999.
32. Tillman, F.A.; Hwang, C.L.; Kuo, W. Optimization techniques for system reliability with Redundancy—A review. *IEEE Trans. Reliab.* **1977**, *26*, 148–155. [[CrossRef](#)]